Pressure-induced water flow through model nanopores

Jacob Goldsmith and Craig C. Martens*

Received 7th May 2008, Accepted 2nd October 2008
First published as an Advance Article on the web 21st November 2008
DOI: 10.1039/b807823h

This paper describes nonequilibrium molecular dynamics simulations of pressure induced transport of liquid water through model nanopores. We consider a simple model for a porous membrane consisting of a slab of water molecules held in a rigid ice structure and penetrated by a pore of nanometer scale dimensions. Both hydrophilic membranes composed of conventional TIP3P water and hydrophobic membranes consisting of modified water with the model partial charges set to zero are treated. Molecular dynamics simulation is employed to investigate the rate of water flow through the pore induced by a pressure difference across the membrane. The results are compared with the predictions of continuum hydrodynamics. We find that the flow rate of water through hydrophilic pores is much less than the continuum predictions, while the flux through hydrophobic pores can significantly exceed the continuum theory. Finally, we show asymmetric behavior in the flux *vs.* pressure difference for a conical nanopore, which thus acts as a Brownian ratchet.

1. Introduction

Fluid flow on the molecular scale is a phenomenon of great current interest. The nanoscale transport properties of water and aqueous solutions have relevance to a range of applications, including the structure and function of membrane channel proteins, separation and purification using nanoporous membranes, and the design of nanofluidic devices. Recent experimental advances have allowed membranes containing nanoscale pores to be synthesized with well-defined structure on the molecular scale. Hinds and coworkers prepared nanoporous membranes constructed from aligned multiwalled carbon nanotubes.[1] Holt and coworkers recently reported measurements of gas and liquid water transport through membranes fabricated from arrays of aligned carbon nanotubes with diameters of less than 2 nm.[2] Pressure-induced water flow through these nanopores can exceed continuum hydrodynamics predictions by orders of magnitude, indicating a strong deviation by these systems from behavior expected from macroscopic theories. The incorporation of pores based on carbon nanotubes into permeable membranes evidently allows nearly frictionless transport that results from their weak interactions with water and their smoothness on the molecular scale. Molecular dynamics simulations of water in carbon nanotubes[3–6] and other nanpores[7–12] have provided qualitative agreement with the experimental measurements and are yielding molecular-level insight into these novel systems.

The properties of nanoscale fluids are highly correlated to the physical nature and functionality of the proximal surface.[13,14] In cavities, the behavior of water has been shown to be highly sensitive to the size of the cavity and the strength of the interaction between water and the cavity walls.[15] Generally, diffusion rates decrease and the viscosity increases as the wet surface area to volume increases,[16] but large flow rates for smooth hydrophilic nanopores have been observed.[6] In pores, the nanoscopic functionality is often categorized as hydrophilic or hydrophobic and influences the flow profile of solutions through the pore.[17]

In this paper, we present molecular dynamics simulations of pressure induced transport of water through model nanopores. We consider a simple model for a porous membrane consisting of a slab of water molecules held in a rigid ice structure and penetrated by a pore of nanometer scale dimensions. Nonequilibrium molecular dynamics simulations are employed to investigate the rate of water flow through the pore induced by a pressure difference across the membrane and the atomic level details of the transport process. The results are compared with the predictions of continuum hydrodynamics.

2. Model systems

We treat pressure-induced flow of liquid water through model nanopores spanning a membrane. We consider a very simple model system for which relevant parameters such as size, shape, and nanopore surface properties can be controlled precisely and the resulting behavior analyzed quantitatively. In particular, we study a family of systems based on pores penetrating a *rigid ice-like membrane*. The membrane in these systems is composed of water molecules (perhaps with modified properties) held fixed in space in an ice Ih structure during the molecular dynamics simulations. Our pore surfaces are structured at the atomic level, but thermal motion of the membrane is ignored. The roles of structure and thermal motion of pores in transport have been considered previously (see, for instance, ref. 18 and 19).

Pores through the membrane are created by removing selected water molecules from the slab of rigid ice composing the membrane. By varying the spatial conditions on the

Department of Chemistry, University of California, Irvine, Irvine, CA 92697-2025, US. E-mail: cmartens@uci.edu

removed water molecules, nanopores with different sizes and geometries can be constructed. Families of membrane/pore systems of varying membrane thickness, pore diameter, and pore shape can be easily generated.

In some of the simulations presented, the molecules comprising the membrane are standard model waters (*e.g.*, TIP3P[20]), and the resulting systems are prototypical hydrophilic pores. We can further modify the pore characteristics, however, by artificially changing the parameters in the water model. For instance, highly hydrophobic nanopores can be constructed by re-setting the partial charges of the membrane water molecules to zero. The propensity for such pores to fill when in contact with an aqueous reservoir can further be tuned by adjusting the van der Waals interaction between the solution waters and the artificial waters comprising the pore (see, *e.g.*, ref. 3,14). Intermediate systems can be produced by systematically varying the partial charges on the atoms in the membrane waters between zero and their physical values, and beyond, to higher values. This model, although not realizable experimentally, allows purely structural effects to be separated from the influence of the electrostatic hydrogen bonding between solution and the surface of the pore.

We model water transport under a pressure difference across a membrane through both symmetric and asymmetric nanopore systems. The symmetric systems consist of a model ice membrane of $L = 2.4$ nm thickness spanned by an approximately cylindrical pore generated by removing water molecules that fall completely or partly within a radial distance R from the z axis perpendicular to the membrane. We consider two cases: small pores with $R = 0.6$ nm and larger pores with $R = 0.9$ nm. Then, for each size, we treat the hydrophilic pore case, with standard TIP3P water[20] comprising the membrane, and the hydrophobic variant with the membrane waters replaced by "NIP3P"—a variant of TIP3P waters with the partial charges set equal to zero. This latter system has the same pore geometry, as defined by the atomic positions in the ice Ih lattice and the van der Waals parameters of the water model, but without the ability to form hydrogen bonds *via* the electrostatic interactions between the partial charges on the pore surface and the mobile waters.

In Fig. 1 and 2 we show snapshots of simulations of water flow through the $R = 0.6$ nm and $R = 0.9$ nm hydrophilic nanopore systems, respectively. The rigid membrane waters are indicated as line drawings.

We also consider an asymmetric system consisting of an approximately conical hydrophilic nanopore generated by removing water molecules from the rigid ice membrane that fall at least partly within a given radial distance $R(z)$ from the z axis that now depends on position along the nanopore. We treat a single system characterized by a conical opening that ranges from $R = 0.6$ nm on one side of the membrane to $R = 1.5$ nm on the other. A snapshot from a simulation using this system is shown in Fig. 3.

3. Simulation methodology

We simulate the flow of water through the model nanopore systems under an imposed pressure difference across the membrane using the method of molecular dynamics.[21–23]

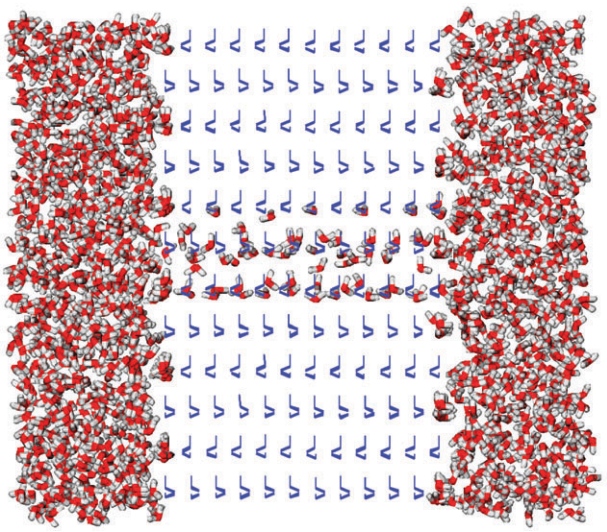

Fig. 1 Model membrane/nanopore system, as described in the text. The membrane thickness is $L = 2.4$ nm, while the pore diameter $R = 0.6$ nm.

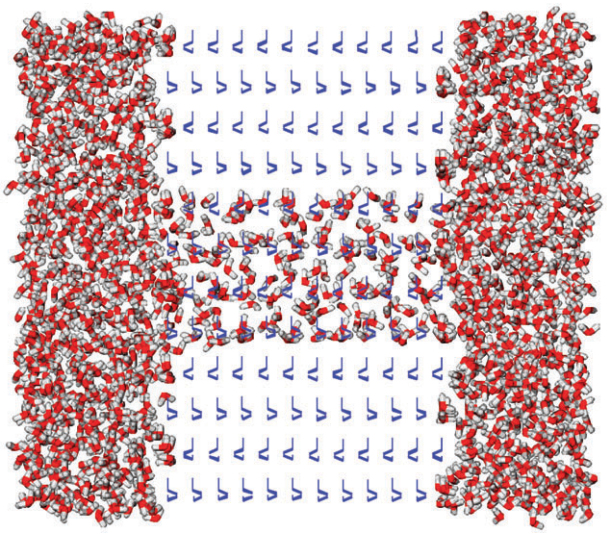

Fig. 2 Same as Fig. 1, but with $R = 0.9$ nm.

The calculations described here are carried out using the NAMD molecular dynamics package, developed by the Theoretical and Computational Biophysics Group in the Beckman Institute for Advanced Science and Technology at the University of Illinois at Urbana-Champaign.[24] Visualization and data analysis are conducted using VMD, a visualization package also available from UIUC.[25]

The water model we employ is the TIP3P potential,[20] which treats water as a rigid molecule with van der Waals interactions and appropriate partial charges located on the atoms. Although simple, this water potential is commonly used when studying large aqueous systems, and is a part of the force field included with the NAMD package. (In later studies, the robustness of our model study results to the water model will be assessed.)

The models we study are finite representations of infinite systems. Unwanted boundary effects are avoided by using periodic boundary conditions,[21–23] where the basic simulation

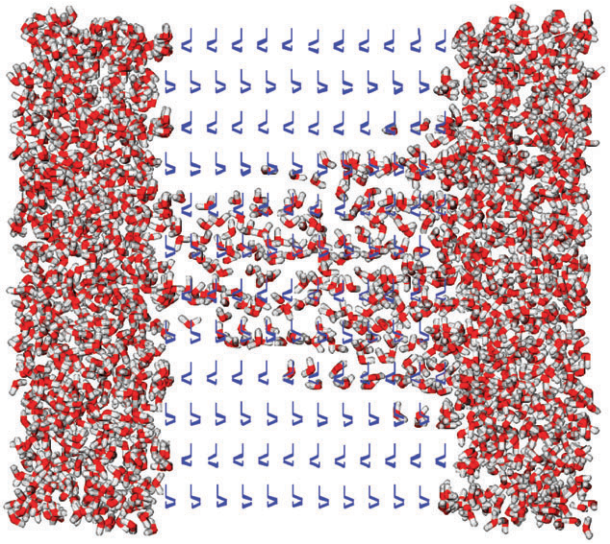

Fig. 3 Asymmetric pore with conical geometry, as described in the text. Membrane thickness is $L = 2.4$ nm. The small opening of the pore has a radius of approximately 0.6 nm, while the radius of the large opening is approximately 1.5 nm.

box is repeated periodically throughout space. Long-range electrostatic interactions between charged particles are treated using the particle-mesh Ewald (PME) method.[23]

We initially equilibrate the systems at constant temperature T and pressure P using a stochastic Langevin approach to control the temperature and a Langevin piston method to control pressure.[24] We equilibrate the initial systems to $T = 300$ K and $P = 1$ barr, respectively. We perform all equilibrations beginning with an ice Ih crystal in a box of dimensions $(a,b,c) = (4.72,4.48,5.43)$ nm, corresponding to the dimensions (x,y,z). We equilibrate at constant (T,P) with the mobile water in contact with the hydrophilic fixed water membrane/pore structure for 1 ns. The x and y dimensions are held constant, while the z dimension varies under the imposed pressure. As the initial ice crystal melts, the volume decreases, leading to a final cell size in the z direction of approximately $c = 5.15$ nm. Subsequent constant T flow simulations are performed at this final constant volume V. We employ the same volume for both the hydrophilic and hydrophobic systems.

Pressure differences across the membrane are imposed by applying external forces to selected atoms in the liquid water reservoir. We apply a constant force in the z direction (defined as the direction along the pore) to the oxygen atoms of water molecules within a fixed distance of approximately 0.3 nm of the left or right boundary of the system. This induces a pressure gradient across the membrane and steady-state flow through the pore after the decay of transient dynamics. The pressure is calculated by computing the total force applied divided by the area $A = ab$ of the membrane unit cell. The system is allowed to come to steady state by running the simulations for an additional 1 ns after equilibration before collecting flow data.

4. Results and discussion

For the cylindrical pore systems, we perform simulations of water transport for a range of negative pressure differences, which induce steady state flow of water in the direction of increasing z. Transport data is collected over 0.5 ns time windows from simulations of systems previously brought to a steady state, as described above. We compute the flux through the pore in molecules per nanosecond and show the results of our simulations for the $R = 0.6$ nm and $R = 0.9$ nm systems in Fig. 4 and 5, respectively. Each figure presents the dependence of flux on pressure difference for both the hydrophilic and hydrophobic pore systems for the given value of R.

We compare our results with the prediction of the Hagen–Poiseuille equation,[26] which gives the volumetric flux Q in terms of the absolute pressure difference ΔP, the pore diameter D, the pore length L, and the dynamic viscosity μ.

$$Q = \frac{\pi D^4}{128\mu}\frac{\Delta P}{L}. \qquad (4.1)$$

For water, $\mu = 10^{-3}$ Pa s. This continuum theory is not expected to be applicable for such small systems. Still, the expression is in reasonable qualitative agreement with the simulations, and is quite close to the hydrophobic pore results for $R = 0.9$ nm. For the smaller $R = 0.6$ nm hydrophobic pore, the simulated flux is higher than the Hagen–Poiseuille equation prediction. The flux through the hydrophilic pores is significantly less than both the hydrophobic pore transport and the Hagen–Poiseuille equation predictions.

In order to understand the dynamical processes of water transport in more detail, we compute the average velocity in the pores as a function of the distance r from the pore axis for a representative absolute pressure difference of $\Delta P = 160$ MPa. These are calculated by determining the velocity of each atom in each of 1000 frames written out during the course of the 0.5 ns simulation and averaging over bins of the radial position within the pore. Only water molecules with z within the inner 2.0 nm of the pore are considered in order to avoid perturbations from the pore openings. Averaging over time is also performed. The results are presented in Fig. 6 and 7 for the $R = 0.6$ nm and $R = 0.9$ nm systems, respectively. These are compared with the theoretical prediction of the

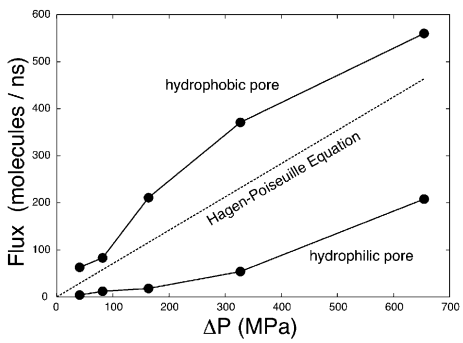

Fig. 4 Water flux *vs.* absolute pressure difference ΔP for the $R = 0.6$ nm nanopore model. Results for both the hydrophilic (TIP3P) membrane and the hydrophobic (NIP3P; see text) membrane are shown. The results are compared with the predictions of Hagen–Poiseuille equation, eqn (4.1).

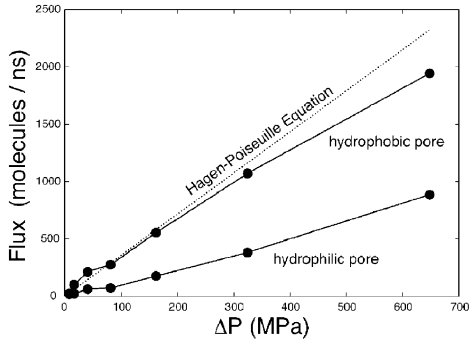

Fig. 5 Same as Fig. 4, but for the $R = 0.9$ nm nanopore system.

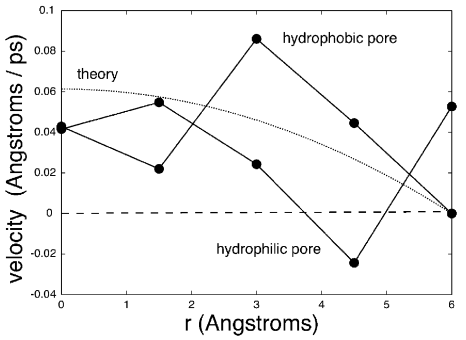

Fig. 6 Average velocity $v(r)$ as a function of radial position r within the $R = 0.6$ nm nanopore system. Results for both the hydrophilic and hydrophobic pore model are shown, and compared with the prediction of continuum hydrodynamics, eqn (4.2). Results are for an absolute pressure difference of $\Delta P = 160$ MPa. See text for discussion.

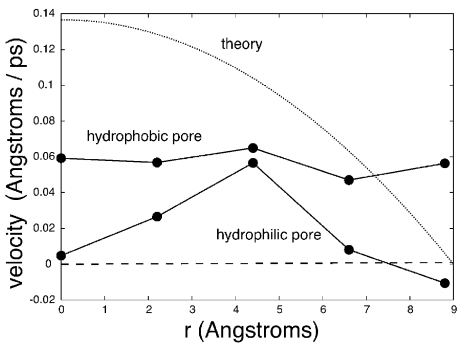

Fig. 7 Same as Fig. 6, but for the $R = 0.9$ nm nanopore system.

position-dependent velocity field derived from solution of the Navier–Stokes equation for flow in a cylindrical pore with stick boundary conditions, which gives[26]

$$v(r) = -\frac{\Delta P R^2}{4\mu L}\left(1 - \left(\frac{r}{R}\right)^2\right). \qquad (4.2)$$

This expression shows the characteristic parabolic velocity profile expected for pressure-driven continuum fluid flow through a cylindrical pipe with stick boundary conditions: the predicted velocity vanishes at the boundary $r = R$, and grows to achieve a maximum along the pore axis, $r = 0$. The Hagen–Poiseuille equation, eqn (4.2), can be derived by integrating this velocity field over the cross sectional area of the pore.

From Fig. 6 and 7 we see that the fluid dynamics theory predicts velocities that are qualitatively of the correct order of magnitude, but does not describe the shape of the distributions well. For these systems, and especially for the smaller $R = 0.6$ nm pore, the atomic motions of the water molecules undergoing transport are very different in character than that of a steady fluid flow. The velocities fluctuate strongly with position, and can even become negative in some cases. This is consistent with qualitative information revealed from viewing movies of the trajectories, which suggest that transport of water through the hydrophilic pore occurs as a biased hopping between relatively stable, solid-like sites rather than by the smooth flow exhibited by a continuum fluid. The thermal velocity

$$v_{\mathrm{th}} = \sqrt{k_{\mathrm{B}}T/m} \cong 3.7 \text{ Å ps}^{-1}$$

for water at $T = 300$, so the instantaneous velocities of atoms resulting from random thermal motion are typically much larger than the net transport velocity down the nanopore. For pores larger than a few molecular diameters in size, the properties of water in the pore becomes bulk-like away from the perturbing effect of the water-pore interface. But for the small systems considered here, the water in the pore is always within a few Angstroms of the pore surface, and its structural and dynamical properties are strongly influenced by interfacial interactions. The ice structure of the hydrophilic pores acts as an optimal template for inducing solid-like structure in the water, which must then be disrupted for transport to occur.

Although the hydrophobic $R = 0.6$ nm pore does not possess the strong hydrogen bonded interactions with water resulting from nonzero partial charges that characterize the hydrophilic system, it still has a structured surface that affects the behavior of vicinal water molecules. The rigid ice structure employed in our model pores is structurally complementary to the liquid water within the tube, even in the absence of strong interactions. Our systems are thus not as smooth as the carbon nanotube bases systems considered experimentally in ref. 1 and 2 or theoretically in ref. 3–6. The ice structure in fact is in a sense optimally rough, as its structure is matched geometrically to the inherent ice-like structure of the water. For the hydrophilic pores, electrostatic interactions will cause the pore wall to act as a template, inducing the water within the pore to adopt a more solid-like structure. This is expected to impede the flow, and animated trajectories of these systems confirms the transport of water in the small hydrophilic pores to be more like biased solid diffusion than fluid flow.

For the larger $R = 0.9$ nm system the velocity profiles are smoother. Neither the hydrophobic nor the hydrophilic systems exhibit the characteristic parabolic distribution, however. For the hydrophilic case, the interfacial interactions propagate through the entire liquid volume, strongly influencing the dynamics of transport. The hydrophobic system exhibits a relatively flat velocity profile which does not vanish at the pore boundary. This indicates that all the water in the pore is transported down the tube with roughly the same average velocity. This is consistent with the slip boundary condition

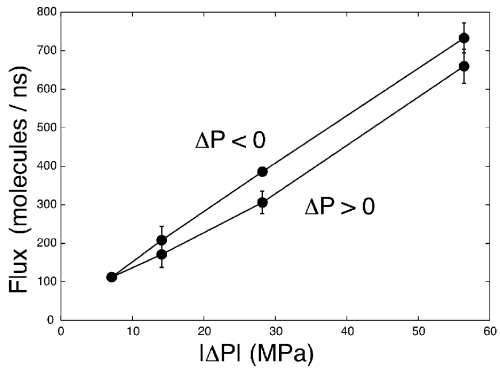

Fig. 8 Water flux *vs.* the absolute difference gradient $|\Delta P|$ for the asymmetric conical nanopore system. The results for both positive and negative pressure differences are shown, as described in the text. Error bars are estimated from the standard deviation of three independent 0.5 ns simulations for each condition.

and plug-like transport proposed in the nanopore systems studied experimentally in ref. 1 and 2. Water–water interactions within the moving fluid are much stronger than the water-interface (TIP3P–NIP3P) interactions, resulting in the collective motion of a plug of liquid water and a nonzero velocity at the interface. The flow rate for the hydrophobic system is not orders of magnitude higher than the corresponding hydrophilic system as seen in the carbon nanotube experiments, however. This result is consistent with the idea that the current system is not as smooth and frictionless as a carbon nanotube pore. Presumably, the actual flow rate obtained is controlled by the precise nature of this residual frictional interaction, suggesting future studies to systematically characterize the effect.

We now consider preliminary results for presure-induced flow in *asymmetric* model nanopores. In Fig. 8 we show data obtained from simulations of pressure-induced flow through the conical pore system illustrated in Fig. 3. Because of the asymmetry of the system, the flux-pressure difference behavior is not required to be symmetric. Indeed, such asymmetric molecular scale systems can act as Brownian ratchets[27,28] and thus exhibit rectification of transport. Recent experiments have shown asymmetry in current–voltage curves generated from the measurement of ion currents through single conical nanopores.[29–31] Fig. 8 indeed demonstrates a small but statistically significant asymmetry of the flux. Here, three 0.5 ns runs were conducted at each pressure gradient and the result averaged. The error bars correspond to the standard deviation of the three runs, and suggests that the observed asymmetry is larger than statistical fluctuations. The flux is higher for a given negative pressure difference $\Delta P < 0$, which corresponds to flow from left to right in Fig. 3. Physically, it is easier to enter the small end and leave the big end than vice versa. An analogy can be drawn with motion on Southern California freeways: fewer traffic jams result when lanes are added to a freeway than when the number of lanes decrease in the direction of traffic flow.

5. Summary

In this paper, we have presented nonequilibrium molecular dynamics simulations of the pressure induced transport of water through model nanopores. Our simulation system consists of a simple model for a porous membrane based on a slab of water molecules constrained in a rigid ice structure spanned by a nanopore of variable size, character, and geometry. Both hydrophilic membranes composed of conventional TIP3P water and hydrophobic membranes consisting of modified water with the model partial charges set to zero were considered. The flux of water through the pore induced by a pressure difference across the membrane was simulated, and the results compared with the predictions of continuum hydrodynamics. We found that the flow rate of water through hydrophilic pores is much less than the continuum predictions, while the flux through hydrophobic pores can significantly exceed the continuum theory. Finally, we showed asymmetric behavior in the flux *vs.* pressure difference for conical nanopores, providing an atomistic realization of a Brownian ratchet.

Acknowledgements

We thank Zuzanna Siwy, Dean Astumian, Gerhard Hummer, and Steve Jaffe for helpful discussions. This work was supported in part by the Institute for Surface and Interface Science (ISIS) at the University of California, Irvine.

References

1 B. J. Hinds, N. Chopra, T. Rantell and R. Andrews, *Science*, 2004.
2 J. K. Holt, H. G. Park, Y. Wang, M. Stadermann, A. B. Artyukhin, C. P. Grigoropoulos, A. Noy and O. Bakajin, *Science*, 2006, **312**, 1034–1037.
3 G. Hummer, J. C. Rasaiah and J. P. Noworyta, *Nature*, 2001, **414**, 188–190.
4 A. Berezhkovskii and G. Hummer, *Phys. Rev. Lett.*, 2002, **89**, 064503–1.
5 A. Kalra, S. Garde and G. Hummer, *Proc. Natl. Acad. Sci. U. S. A.*, 2003, **100**, 10175–10180.
6 S. Joseph and N. Aluru, *Nano Lett.*, 2008, **8**(2), 452–458.
7 O. Beckstein, P. C. Biggins and M. S. P. Sansom, *J. Phys. Chem. B*, 2001, **105**, 12902–12905.
8 R. Allen, S. Melchionna and J. P. Hansen, *Phys. Rev. Lett.*, 2002, **89**, 175502–1.
9 R. Allen, J. P. Hansen and S. Melchionna, *J. Chem. Phys.*, 2003, **119**, 3905–3919.
10 A. Raghunathan and N. R. Aluru, *Phys. Rev. Lett.*, 2006, **97**, 024501.
11 C. Huang, K. Nandakumar, P. Choi and L. Kostiuk, *J. Chem. Phys.*, 2006, **124**, 234701.
12 H. Takaba, Y. Onumata and S.-I. Nakao, *J. Chem. Phys.*, 2007, **127**, 054703.
13 T. Sun, L. Feng, X. Gao and L. Jiang, *Acc. Chem. Res.*, 2005, **38**(8), 644–652.
14 N. Giovambattista, P. G. Debenedetti and P. J. Rossky, *J. Phys. Chem. C*, 2007, **111**, 1323–1332.
15 M. Gordillo, G. Nagy and J. Marti, *J. Chem. Phys.*, 2005, **123**, 054707.
16 Y. Liu, Q. Wang and L. Lu, *Langmuir*, 2004, **20**, 6921–6926.
17 E. Savariar, K. Krishnamoorthy and S. Thayumanavan, *Nat. Nanotechnol.*, 2008, **3**, 112–117.
18 R. F. Cracknell, D. Nicholson and K. E. Gubbins, *J. Chem. Soc., Faraday Trans.*, 1995, **91**, 1377–1383.
19 Q. Cai, M. J. Biggs and N. A. Seaton, *Phys. Chem. Chem. Phys.*, 2008, **10**, 2519–2527.
20 W. L. Jorgensen, J. Chandrasekhar, J. D. Madura, R. W. Impey and M. L. Klein, *J. Chem. Phys.*, 1983, **79**, 926–935.
21 M. P. Allen and D. J. Tildesley, *Computer Simulation of Liquids*, Clarendon Press, Oxford, 1987.

22 *Simulation of Liquids and Solids*, ed. G. Ciccotti, D. Frenkel and I. R. McDonald, North Holland, New York, 1987.
23 D. Frenkel and B. Smit, *Understanding Molecular Simulation*, Academic, New York, 2002, 2nd edn.
24 J. C. Phillips, R. Braun, W. Wang, J. Gumbart, E. Tajkhorshid, E. Villa, C. Chipot, R. D. Skeel, L. Kale and K. Schulten, *J. Comput. Chem.*, 2005, **26**, 1781–1802.
25 W. Humphrey, A. D. and K. Schulten, *J. Mol. Graphics*, 1996, **14**, 33–38.
26 D. J. Tritton, *Physical Fluid Dynamics*, Oxford University Press, Oxford, 1988, 2nd edn.
27 R. D. Astumian, *Science*, 1997, **276**, 917–922.
28 P. Reimann, *Phys. Rep.*, 2002, **361**, 57265.
29 Z. Siwy and A. Fulinski, *Phys. Rev. Lett.*, 2002, **89**, 198103.
30 Z. Siwy, *Adv. Funct. Mater.*, 2007, **16**, 735–746.
31 M. R. Powell, M. Sullivan, I. Vlassiouk, D. Constantin, O. Sudre, C. C. Martens, R. S. Eisenberg and Z. S. Siwy, *Nat. Nanotechnol.*, 2008, **3**, 51.